Vibration Suppression of Thin-Walled Composite Tubes Using Embedded Viscoelastic Layers

Frank M. Belknap
Composite Optics, Inc.
San Diego, California
and
J. B. Kosmatka
Department of Applied Mechanics and Engineering Science
University of California
San Diego, California 92093

Abstract

This paper documents the design and fabrication of a thin-walled composite tube consisting of inner and outer graphite shells with a viscoelastic layer between the shells to provide damping. The graphite shells are fabricated from fabric and unidirectional tape with ply orientations that cause the shells to counter-rotate in opposite directions when subjected to bending or extension. The counter-rotation of inner and outer shells provides a large shear area at the viscoelastic layer, therefore optimizing the damping. Stiffness characteristics of a laminated tube are used to determine ply orientations to maximize damping and structural stiffness. Details of the tube construction are described along with design issues of incorporating viscoelastic layers in a composite laminate. Tests results of the tube with an embedded viscoelastic layer are compared to those of a tube constructed from the same laminate without the damping layer.

Introduction

The need for lightweight, high-strength structures often leads to various vibration problems. Advanced composites offer high stiffness-to-weight ratios, but the levels of structural damping remain relatively low. Viscoelastic materials, which are also lightweight, offer vibration attenuation, but cannot be used as structural elements because of their low stiffness properties. Hybrid composite structures are being designed with layers of viscoelastic materials strategically embedded in composite laminates to control motion due to the vibration.

One example of a hybrid composite structure, that can provide high damping levels, is a thin-walled composite tube consisting of a viscoelastic layer embedded between inner and outer graphite/epoxy shells. The graphite/epoxy shells are fabricated from woven cloth and unidirectional tape. The plies of the unidirectional tape are oriented so the fibers wrap

spirally around the inner shell, and wrap in an opposite (or opposing) spiral in the outer shell. The application of either an extensional, bending, or shear load to the tube ends will produce relative twisting between the inner and outer shells since the shells are rotating in opposite directions. This relative twisting will induce significant shear strain levels in the viscoelastic material, thus producing a large amount of useful structural damping.

If the inner and outer shells of the tube were made of an isotropic material, then the application of either an axial or flexure load would produce tube extension or bending, respectively, but with no relative twisting. This bending-action will produce very low shear levels within the viscoelastic core away from the neutral axis. Studies have shown [1,2] that the effectiveness of this type damping treatment is extremely limited due to the small shear-strain areas. Because the two shells of the current composite design are rotating in opposite directions, shear strain is produced in the entire viscoelastic layer. This large shear area is due to the mechanical advantage of the relative rotational of the two shells acting independently.

The application of an axial load on a tube with isotropic shells would produce shear in the viscoelastic layer if the two shells are only coupled in the axial direction by the viscoelastic layer. This load path will result in high damping but the tube will have low structural stiffness in the axial direction due to the soft viscoelastic layer. The soft core material will react in series with the two stiffer shells resulting in a low system stiffness. Other designs have incorporated the use of viscoelastic layers with composite shells but still requiring one shell to be the primary structural member [3]. With the current composite design developed in the present paper, the two shells twist oppositely when subjected to loading which causes both shells to experience the same length change. Thus, the ends of both shells are coupled in the axial direction and they support the entire axial load without the soft viscoelastic core reducing the system stiffness. Only the rotational degree-of-freedom at both ends of the tube needs to remain unconstrained leaving the axial stiffness unaffected.

The application of damping to spacecraft structures has significant impacts on increased reliability and reduced costs associated with launch and extended operation [4]. The material selection for the current composite design is based upon possible applications for satellite systems. The matrix system used in the graphite/epoxy material must be capable of withstanding the temperature extremes associated with space environments. The viscoelastic material must also be compatible with this resin system. Another area of concern is the possibility of contamination by these types of materials in a space environment.

The graphite material is a fiber type T-300 pre-impregnated with a Hysol #934 resin system that cures at 350 degrees Fahrenheit. The viscoelastic damping material is 3M Scotchdamp SJ-2015X Viscoelastic Polymer Type 1210. This material is provided by 3M Corporation in a standard thickness of 10 mils (.010 inches). The stiffness properties for the viscoelastic material are provided by 3M product information [5]. Outgassing tests were

conducted by the Boeing Aerospace Company [6] on this material and proved it to be acceptable for space applications. A series of structural tests were conducted to verify that the chemical composition of the viscoelastic material did not reduce the mechanical properties of the graphite/epoxy material [7].

Theoretical Development

The stiffness properties of a laminated composite tube are studied so that the ply orientations which maximize the extension-torsion coupling and shear strain in the viscoelastic layer can be determined. Consider a long slender beam of length L acted upon by end forces and moments. A Cartesian coordinate system (x,y,z) and corresponding displacements (u,v,w) are defined where x and y define the cross-section plane and z defines the axial direction. See Fig.1 for further details. The displacement field of a point on the deformed beam can be written in its most general form by assuming that it is a linear combination of global functions that represent extension, bending, and twisting of the tube and local functions that represent generalized warping of the cross-section:

$$\begin{aligned} u(x,y,z) &= u_o(z) - y\theta_o(z) + \psi_x(x,y), \\ v(x,y,z) &= v_o(z) + x\theta_o(z) + \psi_y(x,y), \\ w(x,y,z) &= w_o(z) - x\theta_y(z) + y\theta_x(z) + \psi_z(x,y). \end{aligned} \qquad (1.a\text{-}c)$$

where u_o, v_o, and w_o represent z-dependent displacements in the x, y, and z directions, respectively, ϕ_x, ϕ_y, and θ_o represent rotations about the x, y, and z axes respectively, and ψ_x, and ψ_y represent warping within the cross-section plane and ψ_z is the warping out of the cross-section plane. Assuming a two-dimensional strain state, one can derive the final form of the z-dependent functions as;

$$\begin{aligned} u_o(z) &= \frac{\kappa_x}{2} z^2, \quad & \theta_x(z) &= \kappa_y z, \\ v_o(z) &= -\frac{\kappa_y}{2} z^2, \quad & \theta_y(z) &= \kappa_x z, \\ w_o(z) &= e\, z, \quad & \theta_o(z) &= \theta\, z, \end{aligned} \qquad (2.a\text{-}f)$$

where e, κ_x, κ_y, and θ represent the extension strain, the bending curvatures of the beam in the x-z and y-z planes, and the elastic twist per unit length, respectively. The six strain components of the beam, which

fully account for warping (deformation) within the cross-section, are calculated using Eqns. (1) and (2)

$$\begin{aligned} \varepsilon_{xx} &= \psi_{x,x}\,, & \gamma_{yz} &= x\,\theta + \psi_{z,y}\,, \\ \varepsilon_{yy} &= \psi_{y,y}\,, & \gamma_{xz} &= -y\,\theta + \psi_{z,x}\,, \\ \varepsilon_{zz} &= e - x\kappa_x + y\kappa_y\,, & \gamma_{xy} &= \psi_{x,y} + \psi_{y,x}\,, \end{aligned} \qquad (3.a\text{-}f)$$

The determination of local cross-section deformation functions (ψ_x, ψ_y, ψ_z) is based upon using a separation of variables solution technique combined with the Ritz method assuming that the warping functions can be expressed as a linear combination of unknown functions that are proportional to the axial strain, bending curvatures, and twist rate, i.e.;

$$\begin{aligned} \psi_x &= e\,\psi_x^{(1)} + \kappa_x\,\psi_x^{(2)} + \kappa_y\,\psi_x^{(3)} + \theta\,\psi_x^{(4)} \\ \psi_y &= e\,\psi_y^{(1)} + \kappa_x\,\psi_y^{(2)} + \kappa_y\,\psi_y^{(3)} + \theta\,\psi_y^{(4)} \qquad (4.a\text{-}c) \\ \psi_z &= e\,\psi_z^{(1)} + \kappa_x\,\psi_z^{(2)} + \kappa_y\,\psi_z^{(3)} + \theta\,\psi_z^{(4)}\,. \end{aligned}$$

Since the geometry and material properties of the tube are constant with respect to the z-axis, the current problem reduces to a two-dimensional elasticity problem, where the only unknowns are the warping functions. Since these functions are only dependent upon the cross-section coordinates (x,y), this elasticity problem can be solved by developing special two-dimensional finite elements for studying the cross-section warping behavior. Each lamina (including the viscoelastic layer) is discretized into a series of subregions (finite elements) where the warping within each subregion is described using a bi-quadratic isoparametric interpolation function;

$$\begin{aligned} \psi_x &= [N(x,y)]\{\Psi_x\} \\ \psi_y &= [N(x,y)]\{\Psi_y\} \qquad (5.a\text{-}c) \\ \psi_z &= [N(x,y)]\{\Psi_z\}\,. \end{aligned}$$

The strains are written in matrix form in terms of the unknown displacement functions and the axial strain, bending curvatures, and twist rate;

$$\{\varepsilon\} = [B]\{\Psi\} + [f_b]\{b\} \qquad (6.a)$$

where

$$[B] = \begin{bmatrix} N(x,y)_{,x} & 0 & 0 \\ 0 & N(x,y)_{,y} & 0 \\ 0 & 0 & 0 \\ 0 & 0 & N(x,y)_{,y} \\ 0 & 0 & N(x,y)_{,x} \\ N(x,y)_{,y} & N(x,y)_{,x} & 0 \end{bmatrix}, \tag{6.b}$$

$$\{\Psi\}^T = \left\{ \{\Psi_x\}, \{\Psi_y\}, \{\Psi_z\} \right\} \tag{6.c}$$

$$[f_b] = \begin{bmatrix} 0 & 0 & 0 & 0 \\ 0 & 0 & 0 & 0 \\ 1 & -x & y & 0 \\ 0 & 0 & 0 & x \\ 0 & 0 & 0 & -y \\ 0 & 0 & 0 & 0 \end{bmatrix}, \tag{6.d}$$

and

$$\{b\}^T = \left\{ e,\ \kappa_\xi,\ \kappa_\eta,\ \theta \right\}. \tag{6.e}$$

The principle of minimum potential energy is given as

$$\delta\Pi = \sum_{i=1}^{n} \delta U^{(i)} - \delta W_e^{(i)} = 0 \tag{7}$$

where n is the number of subregions. $dU^{(i)}$ is the variation of the strain energy with respect to the unknown local deformations of the i^{th} subregion given by

$$\delta U^{(i)} = \int_0^L \int_{A^{(i)}} \left\{ \delta\varepsilon^{(i)} \right\}^T \left[C^{(i)} \right] \left\{ \varepsilon^{(i)} \right\} dA^{(i)}\, dz, \tag{8.a}$$

and $\delta W_e^{(i)}$ is the variation of the work of external forces of the i^{th} subregion that results from the applied tractions on the beam ends. This virtual work expression will reduce to zero since both the stresses and the local cross section deformations are assumed to be independent of the axial coordinate (z). A set of linear algebraic equations for determining the local cross section deformations in terms of $\{b\}$ is obtained by substituting Eqns. (6) and (8.a) into Eq. (7) and carrying out the integration over the beam volume. Writing this set of equations for the i^{th} subregion;

$$\left[K^{(i)}\right]\left\{\psi^{(i)}\right\} + \left[F_b^{(i)}\right]\{b\} = \{0\} \tag{9}$$

where the stiffness matrix is defined as

$$\left[K^{(i)}\right] = L\int_{A^{(i)}}\left[B^{(i)}\right]^T\left[C^{(i)}\right]\left[B^{(i)}\right] dA^{(i)} \tag{10.a}$$

and the force matrix is presented as

$$\left[F_b^{(i)}\right] = L\int_{A^{(i)}}\left[B^{(i)}\right]^T\left[C^{(i)}\right]\left[f_b\right] dA^{(i)} \ . \tag{10.b}$$

Since both the stiffness matrix ($[K^{(i)}]$) and the force matrix ($[Fb^{(i)}]$) are linearly dependent upon the beam length (L), then the calculated local deformations functions are length independent and (L) can be dropped from the above equations. Unit solutions for the local deformations (ψ_x, ψ_y, ψ_z) can be calculated for each of the four cases of $\{b\}$ by setting the appropriate value in the array $\{b\}$ equal to unity and the remaining three to zero. Thus, the calculated deformation functions can be written in matrix form as

$$\left\{\psi^{(i)}\right\} = \left[\overline{\psi^{(i)}}\right]\{b\} . \tag{11}$$

where each of the four columns of $[\psi^{(i)}]$ are the unit local deformations associated with the four cases of $\{b\}$. Thus, the calculated functions for the first case represent the local deformations as a result of applied unit axial strain (e) with dimensional units of length per unit axial strain. Similarly, the second and third cases define the local deformation associated with applied bending curvatures (κ_x, κ_y) with dimensional units of length per unit bending curvature. Finally the fourth case describes the local deformation from applied twist rate (θ) with dimensional units of length per unit twist rate. Similarly, the stress components of the i^{th} subregion can be expressed in terms of a set of unit stresses and $\{b\}$ by substituting Eqns. (15) and (9) into (2.a)

$$\left\{\sigma^{(i)}\right\} = \left[\overline{\sigma^{(i)}}\right]\{b\} , \tag{12}$$

where

$$\left[\overline{\sigma^{(i)}}\right] = \left[C^{(i)}\right]\left[\left[B^{(i)}\right]\left[\overline{\psi^{(i)}}\right] + \left[f_b\right]\right] . \tag{13}$$

Finally, the calculated stress components are substituted into the four cross-section equilibrium equations in order to express (e, θ, κ_x, κ_y) in terms of the applied axial force, twist moment, and bending moments:

$$\int_A \sigma_{zz}\, dA = P, \qquad \int_A x\, \sigma_{zz}\, dA = -M_y,$$
$$\int_A y\, \sigma_{zz}\, dA = M_x, \qquad \int_A (y\, \tau_{xz} - x\, \tau_{yz})\, dA = M_z, \tag{14}$$

Numerically integrating the stress over each subregion that comprises the cross-section allows one to study the extension-bend-twist coupling behavior of the <u>constrained</u> tube;

$$\begin{bmatrix} K_{11} & K_{12} & K_{13} & K_{14} \\ K_{12} & K_{22} & K_{23} & K_{24} \\ K_{13} & K_{23} & K_{33} & K_{34} \\ K_{14} & K_{24} & K_{34} & K_{44} \end{bmatrix} \begin{Bmatrix} e \\ \kappa_x \\ \kappa_y \\ \theta \end{Bmatrix} = \begin{Bmatrix} P \\ M_y \\ M_x \\ M_z \end{Bmatrix} \tag{15}$$

Inverting the above relationship, one can study the coupling behavior of an <u>unconstrained</u> bar;

$$\begin{bmatrix} a_{11} & a_{12} & a_{13} & a_{14} \\ a_{12} & a_{22} & a_{23} & a_{24} \\ a_{13} & a_{23} & a_{33} & a_{34} \\ a_{14} & a_{24} & a_{34} & a_{44} \end{bmatrix} \begin{Bmatrix} P \\ M_y \\ M_x \\ M_z \end{Bmatrix} = \begin{Bmatrix} e \\ \kappa_x \\ \kappa_y \\ \theta \end{Bmatrix} \tag{16}$$

Applying an axial force (P) produces extension as a well as bending and twist that satisfy:

$$\frac{\kappa_x}{e} = \frac{a_{12}}{a_{11}}, \qquad \frac{\kappa_y}{e} = \frac{a_{13}}{a_{11}}, \qquad \frac{\theta}{e} = \frac{a_{14}}{a_{11}}. \tag{17}$$

Formulation of Ply Orientation

The cross-section stiffness properties for the tube are examined as a function of the unidirectional tape ply angles ϕ. The ply angle ϕ is defined as zero when the fibers in the ply align with the axial direction (z) of the tube. For stability purposes with this design, the fabric plies are maintained with the fibers oriented at both 0 and 90 degrees. The stiffness properties of the composite tube are sensitive to the orientation of the unidirectional

tape ply angles ϕ. As expected, the torsional stiffness (GJ) of the tube is maximized with ply angles of ± 45 degrees and minimized at 0 and 90 degrees. Both the axial stiffness (EA) and bending stiffness (EI) are maximized with ply angles at 0 degrees and minimized at 90 degrees. A graphical depiction of this ply angle sensitivity is illustrated in Figure 2. Torsional, axial, and bending stiffness are plotted as a function of the unidirectional ply angles ϕ

The coupling of twist to applied extension is evident by the a_{14} term within [a]. The coupling of twist to extension is maximized when the unidirectional tape plies are oriented at an angle of 30 degrees. At this ply angle, the tube undergoes a large amount relative twist displacement, but the tube also suffers a significant reduction in both axial and bending stiffness. Since the tube is designed to have a primary load path in the axial direction, the axial stiffness needs to be monitored as well as the extension-twist coupling. Optimizing the shear between the two shells while maintaining structural stiffness is accomplished by comparing the extension-twist/extension ratio of the composite tube for varying ply angles ϕ. The value of a_{14}/a_{11} is the ratio of extension-twist coupling to extensional stiffness. The extension-twist/extension ratio versus ply orientation is plotted in Figure 3. This ratio is extremely sensitive to ply orientation and is maximized at an angle of 15 degrees.

To evaluate the effect the ply angle has on the damping of the tube, the shear stress within the viscoelastic must be examined. The maximum shear stress shown in Figure 4 as a function of ϕ is at a maximum for a 25 degree ply angle. But once again, optimizing the damping using this method would result in a penalty in structural stiffness. The amount of damping provided through matrix shear deformation of just the graphite/epoxy plies was not considered within this study. The orientation of the plies without a viscoelastic layer provides a supplemental damping mechanism to the laminate [8]. This effect is not accounted for in this analysis since its contribution will be small for a fiber-dominated design such as this one.

Tube Construction

The number of plies in the laminate were determined before the the cross-section properties was analyzed for various ply angles. The types of materials and placement within the laminate were chosen for their desired characteristic behavior. Figure 5 depicts the order of ply sequencing within the entire laminate. The fabric material is placed in the inner and outer most plies of the laminate to provide hoop stiffness to the structure. The hoop stiffness is required because of the low transverse tension capabilities of the viscoelastic layer in the center of the laminate. Large relative displacements between the inner and outer shells in the radial direction will result in a delamination at the graphite-to-viscoelastic interface.

Two plies of the unidirectional tape are used in each of the shells next to the viscoelastic layer. The use of unidirectional graphite material ensures the properly designed extension-bend-twist coupling behavior necessary to maximize damping and yet maintain structural stiffness. For this particular phase of the study, no other combinations of ply distribution or materials were examined.

The mandrel for the lay-up is a 60 inch long by 2.5 inch outer diameter solid aluminum round bar. The mandrel is hand polished to remove any surface imperfections then a releasing agent applied. The first ply is the fabric pre-cut to the required size. The next two plies are the unidirectional tape cut in a manner that maintains continuous fibers the length of the tube. The width of the unidirectional tape is the circumference of the mandrel including preceding plies times an angle of 15 degrees. When these fibers are then placed at 15 degrees to the tube's longitudinal axis and spirally wrapped, the edges of the ply come into contact with one another.

The fabric and two plies of tape create the inner shell of the tube. The unbalanced laminate of this shell will result in the extension-bend-twist coupling that is desired for this design. For this particular application, the viscoelastic damping layer is applied directly to the graphite/epoxy material before it is cured. The damping material selected acts as though it is a pressure-sensitive adhesive and requires only nominal pressure at room temperature to effect a good bond. Special care is required when handling the damping layer to avoid creating a void between this material and the graphite/epoxy layers. To reduce the tackiness of the viscoelastic layer, the damping material should be cooled to 30 degrees Fahrenheit before handling it.

The construction of the outer shell is accomplished the same way as the inner shell. The width of the unidirectional tape and fabric takes into account the increase in the circumference due to the additional preceding plies. The angle of orientation for the unidirectional fibers is in the opposite direction of those for the inner shell. This ensures that the outer shell extension-bend-twist coupling is in the opposite direction from the inner shell.

Once the final ply of the laminate is applied, the tube is wrapped with a teflon film. A layer of shrink wrap tape is applied in a spiral manner to provide uniform pressure during the cure cycle. The shrink wrap and teflon film are perforated to allow excess resin to bleed out of the laminate. A bleeder cloth is wrapped around the tube to absorb any excess resin during the cure cycle.

The cure cycle consists of an increase in temperature from room temperature to 350 degrees Fahrenheit in one hour. The cure temperature of 350 degrees is then held for an additional two hours. The reduction in temperature back to room ambient requires one more hour. The part is

removed from the oven then cooled in a freezer to contract the size of the aluminum mandrel. The composite tube then easily slides off the cold mandrel.

Test Results

A design study was conducted to compare a baseline design without viscoelastic material to the composite construction with the damping layer. The plies of graphite/epoxy fabric and tape are identical for the two laminates. The only difference between the two designs is the absence of the damping layer in the baseline configuration. Other studies [9] have been conducted to analyze the effects of embedded damping layers but they examined the effects of replacing stiffness material with damping material. By maintaining the same number and orientation of plies within the laminates of both tube designs, the direct effect of embedding a damping layer can be quantified.

Measurements were made by the impact-hammer modal-test method with the specimen suspended in the near free-free boundary condition. To simulate the free-free boundary condition, the tubes are suspended in the vertical position by a string. Damping is measured using the half-power band-width method.
The first natural frequencies are similar for the tubes with or without the viscoelastic core. The first mode for the tube without the viscoelastic core is 455 Hertz, while the tube with the viscoelastic core is 400 Hertz. Damping in the first mode for the tube without the viscoelastic core is 0.6 percent. A damping value of 4.3 percent is present in the first mode of the tube with the embedded viscoelastic layer. Frequencies and damping measurements for the axial modes will not be made until end fittings are fabricated to couple the stiffness of the two shells with the viscoelastic core. It is important to note that the tube is designed in a state of axi-symmetric extension, but tested in a state of bending. Comparable results are expected for the load case of extension as obtained from the bending test.

Conclusions

The analytical techniques described in this paper enabled the placement of a viscoelastic core and ply orientations of two shells, optimizing the damping in combination with overall structural stiffness. The test results show a reduction of frequency from 455 to 400 Hertz with the addition of the viscoelastic layer. A majority of the reduction can be attributed to the increase in the mass of the tube from the additional material. The evaluation of the ply orientations within the composite design allows effective use of the damping material with the smallest penalty in stiffness. For a small reduction in stiffness, the damping in the first mode is increased over 7 times by optimizing ply angles and embedding a viscoelastic layer.

References

1) Lall, A. K., Asnani, N. T. and Nakra, B. C., "Damping Analysis of Partially Covered Sandwich Beams," Journal of Sound and Vibration, 1988, Vol. 123 No. 2, pp. 247-259.

2) Johnson, C. D., Kienholz, D. A. and Rogers, L. C., "Finite Element Prediction of Damping in Beams with Constrained Viscoelastic Layers," Shock and Vibration Bulletin, No. 51, May 1981, pp. 78-81.

3) Bronowicki, A. J. and Diaz, H. P., "Analysis, Optimization, Fabrication and Test of Composite Shells with Viscoelastic Layers," paper presented at the Damping '89 Conference, West Palm Beach, Florida, Feb. 1989, pp. GCA1-GCA21.

4) Stahle, C. V. and Staley, J. E., "Application of Damping to Spacecraft Structures," 29th National SAMPE Symposium, April 3-5, 1984, pp. 185-194.

5) 3M Product Information, Scotchdamp SJ-2015X Type 1210, Structural Products Department, St. Paul MN.

6) Ikegami, R., Johnson D. W., Walker, W. J., and Beck, C. J., "The Application of Viscoelastic Passive Damping To Satellite Equipment Support Structures," Journal of Vibration, Acoustics, Stress, and Reliability in Design, 1985, pp. 1-8.

7) Belknap, F. M., "Vibration Reduction of Composite Structures Using Constrained Layer Damping Techniques," Proceedings of the 32nd AIAA/ASME/AHS/ACSE Structures, Structural Dynamics, and Materials Conference, 1991, pp 2391-2396.

8) Andriulli, J. B., "Measured Damping and Modulus of Composite Cylinders," paper presented at the Damping '89 Conference, West Palm Beach, Florida, Feb. 1989, pp. BCC1-BCC26.

9) Barrett, D. J., "A Design for Improving the Structural Damping Properties of Axial Members," paper presented at the Damping '89 Conference, West Palm Beach, Florida, Feb. 1989, pp. HCB1-HCB18.

Figure 1. Coordinate System

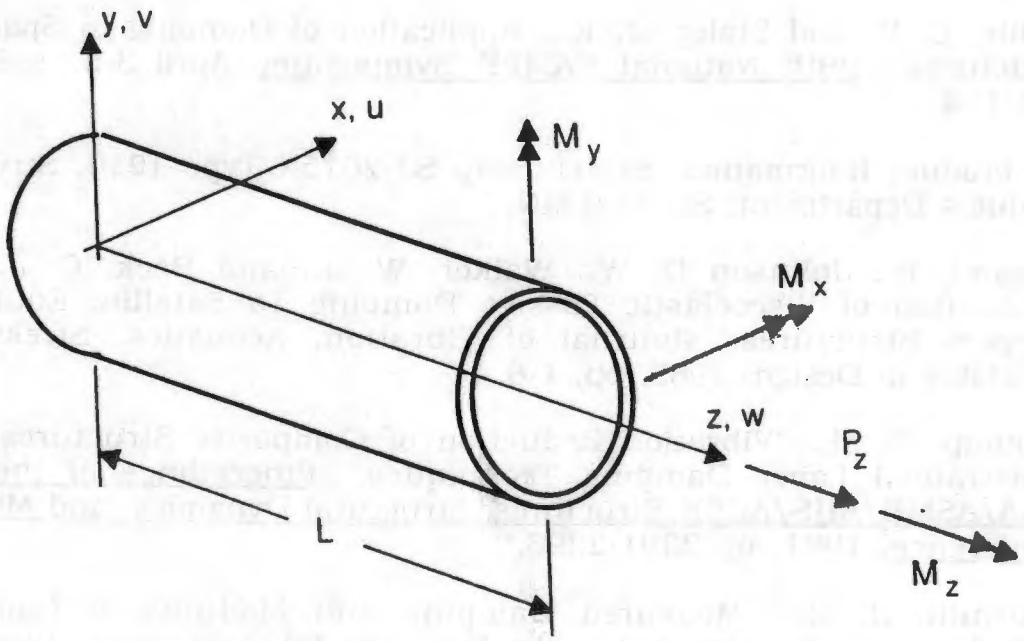

Figure 2. Torsional, Axial, and Bending Stiffness versus Unidirectional Ply Angle

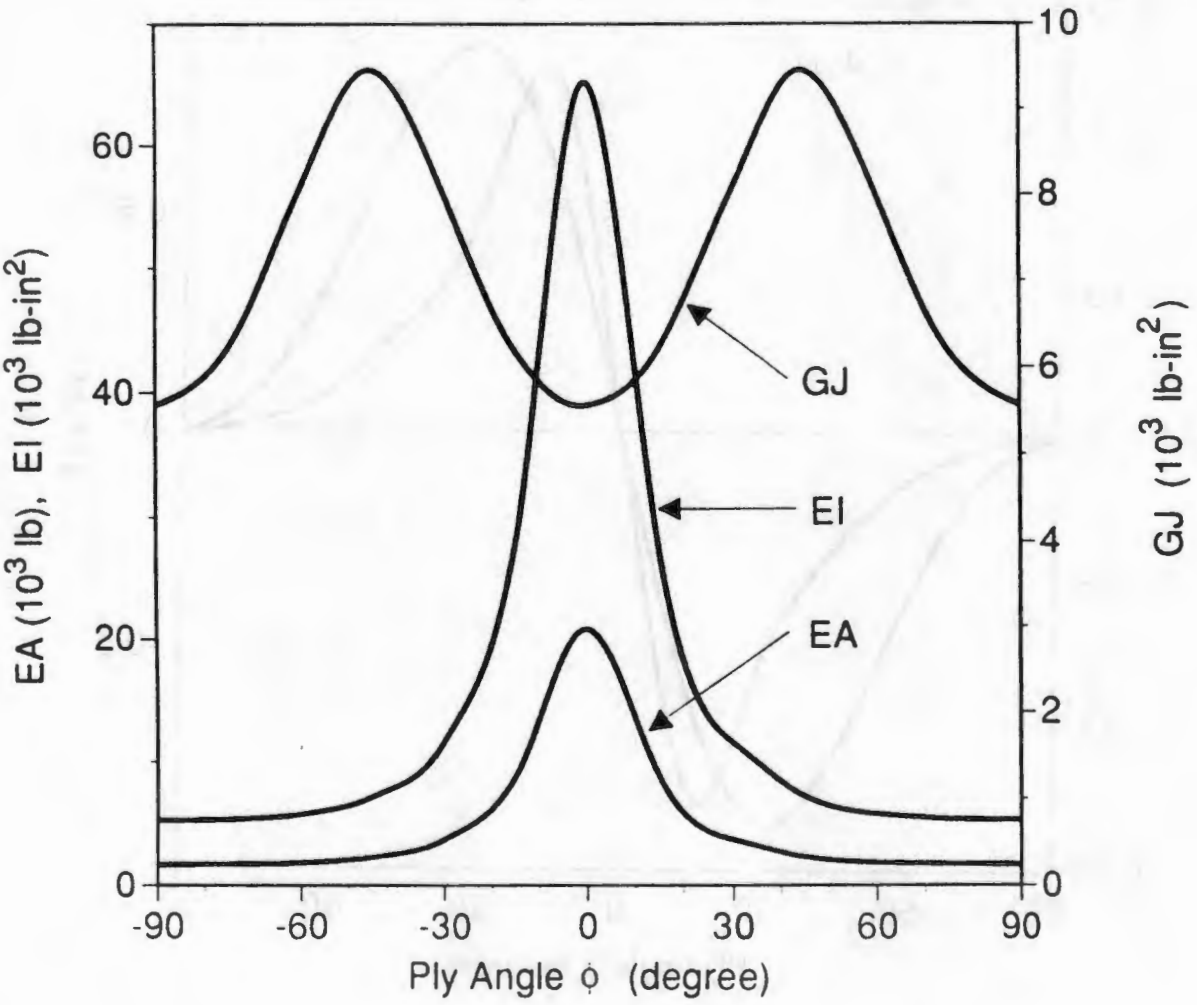

Figure 3. Extension-Twist/Extension Ratio versus Unidirectional Ply Angle

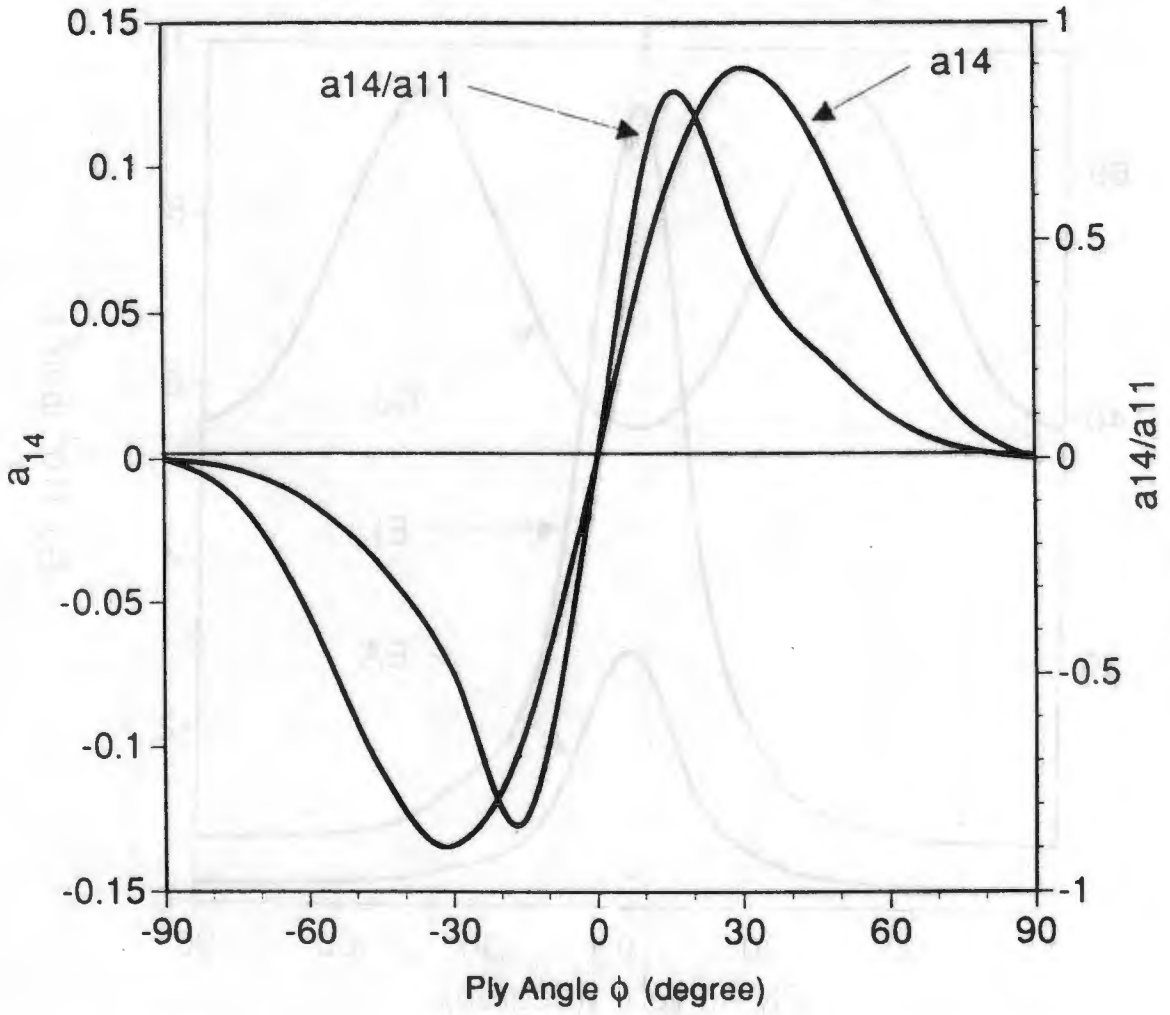

Figure 4. Maximum Shear Stress in Core versus Unidirectional Ply Angle

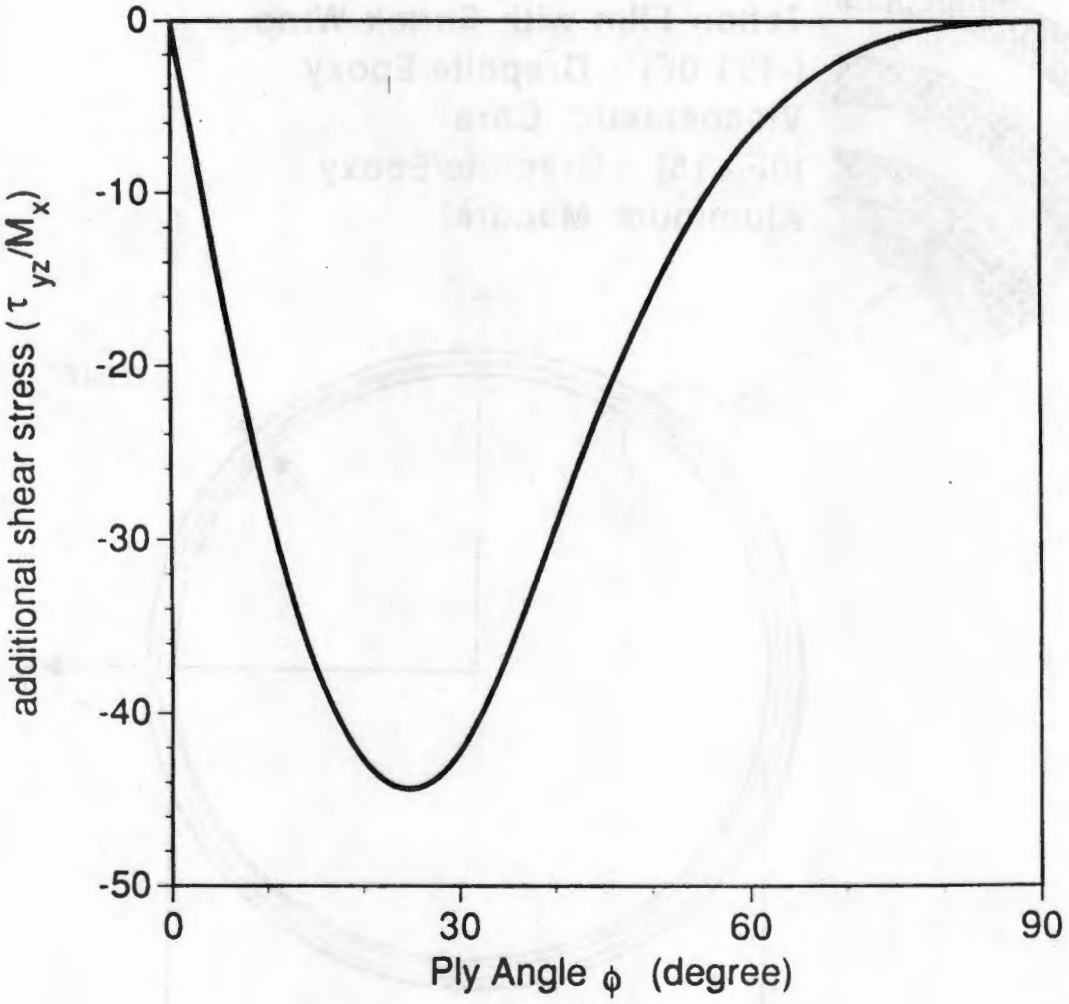

Figure 5. Ply Sequencing of Laminate